Characterization of the tetrodotoxin-resistant Na^+ channel, $Na_v1.9$, in mouse dorsal root ganglion neurones

Hiroshi Maruyama, Mitsuko Yamamoto, Yoshiaki Ohishi, Tomoya Matsutomi, Taixing Zheng, Yoshihiro Nakata*, John N. Wood† and Nobukuni Ogata

*Department of Neurophysiology and *Department of Pharmacology, Graduate School of Biomedical Sciences, Hiroshima University, Hiroshima, 734-8551, Japan and †Department Biology, University College, London WC1E 6BT, United Kingdom*

Corresponding author N. Ogata: Department of Neurophysiology, Graduate School of Biomedical Sciences, Hiroshima University, Hiroshima 734-8551, Japan.

Email: ogatan@hiroshima-u.ac.jp

The Na^+ channel isoform, $Na_V1.9$ (NaN/SNS2), is preferentially expressed in small neurones of the dorsal root ganglia and thought to mediate a novel tetrodotoxin-resistant (TTX-R) Na^+ current. We investigated properties of the Na^+ current mediated by $Na_V1.9$ (I_{NaN}) using whole-cell patch-clamp recording. To isolate I_{NaN} from a heterogeneous TTX-R Na^+ current that also contained another type of TTX-R Na^+ current mediated by $Na_V1.8$ (SNS/PN3), we used $Na_V1.8$-null mutant mice. Since F^- that had been used as an internal anion in earlier studies was shown to produce negative shifts of the activation and inactivation kinetics of I_{NaN}, I_{NaN} was recorded with Cl^- as an internal anion. The activation threshold for I_{NaN} was about 20 mV more negative than that for other Na^+ currents, activation and inactivation were extremely slow giving rise to a persistent Na^+ current, and the peak amplitude was too small (less than 0.5 nA) to carry an action potential generation. Thus, $Na_V1.9$ is a 'background' Na^+ channel that probably regulates excitability at a subthreshold voltage range and influences spike discharges that are predominantly mediated by other Na^+ channels. Since functional expression of I_{NaN} declined with time after dissociation and recovered in step with concurrent glial outgrowth, $Na_V1.9$ is an 'inducible' Na^+ channel. Moreover, $Na_V1.9$ is a 'kindling' Na^+ channel, since the peak amplitude of I_{NaN} under whole cell patch clamp recording started to increase explosively after a variable period of delay, as if 'inactive' or 'silent' $Na_V1.9$ channels were unmasked. Such an unusual increase of the current was not observed under nystatin-perforated recording and was prevented by ATP supplemented in the patch internal solution, indicating that the rupture of the

patch membrane affected the normal behavior of $Na_V1.9$. The inducible and kindling properties of I_{NaN} may provide an additional insight into the plasticity of Na^+ channels that are related to pathological functions of Na^+ channels accompanying abnormal pain states.

Voltage-gated Na^+ channels play critical roles in electrogenesis in most excitable cells. At least seven isoforms of Na^+ channel α–subunits are known to express in the dorsal root ganglion (DRG) (Goldin, 2001). Smaller types of DRG neurones that extend unmyelinated C fibres or thinly myelinated A_δ fibres mainly conduct noxious information. Larger types of DRG neurones that extend myelinated A_β fibres normally conduct innocuous sensation. These distinct types of DRG neurones express a unique repertoire of Na^+ channel isoforms thought to mediate different modalities of sensation.

The two Na^+ channel isoforms, $Na_v1.8$ (SNS/PN3) (Akopian et al. 1996) and $Na_v1.9$ (NaN/SNS2) (Dib-Hajj et al. 1998), are both preferentially expressed in small DRG neurones, suggesting their roles in nociception. Interestingly, these two isoforms contain a structural motif common to tetrodotoxin-resistant (TTX-R) Na^+ channels (Satin et al. 1992; Akopian et al. 1996; Dib-Hajj et al. 1998). $Na_v1.9$ is expressed in non-peptidergic IB4-positive small DRG neurones that are dependent on glial-derived neurotrophic factor (GDNF), whereas $Na_v1.8$ is preferentially expressed in peptidergic IB4-negative small DRG neurones that are dependent on nerve growth factor (NGF) (Fjell et al. 2000). Therefore, $Na_v1.8$ and $Na_v1.9$ may play distinct functional roles in the process of nociception.

Although the property of the Na^+ current mediated by $Na_V1.8$ (I_{SNS}) and its functional role in nociception are relatively well understood (Elliott & Elliott, 1993; Ogata and Tatebayashi, 1993; Gold et al. 1996; Tanaka et al. 1998; Akopian et al. 1999; Lai et al.

2000; Laird et al. 2002), little has been known about the Na^+ current mediated by $Na_V1.9$ (I_{NaN}). In an attempt to observe I_{NaN} in isolation, we constructed $Na_V1.8$-null mutant mice, which are devoid of I_{SNS} (Akopian et al. 1999). A subsequent patch-clamp study utilizing this mutant mice unveiled an additional TTX-R Na^+ current that is dependent on $Na_v1.9$ transcript (Cummins et al. 1999). In addition, Dib-Hajj et al. (2002) succeeded in functional expression of $Na_V1.9$ in an exogenous system. I_{NaN} showed much slower kinetics and a more negative activation threshold than I_{SNS}, thus giving rise to a persistent Na^+ current at subthreshold voltages. To search for $Na_V1.9$ function further, we also performed patch-clamp experiments on acutely dissociated DRG neurones from $Na_V1.8$-null mutant mice. We now report on the unusual properties of $Na_v1.9$, which has not been reported for any other known Na^+ channels.

METHODS

Isolation of single DRG neurones and cell culture

All procedures were carried out under protocols approved by Hiroshima University Animal Ethics Committee. Dissociated single DRG neurones and their culture were prepared as described by Fujikawa et al. (1997). Adult mice were sacrificed by cervical dislocation under ethyl-carbamate (3mg/g) anesthesia. The DRGs from all spinal levels were removed from wild type and $Na_v1.8$-null mutant mice and desheathed in ice-cold Ca^{2+}/Mg^{2+}-free phosphate-buffered saline. The isolated DRGs were enzymatically

digested at first with 0.2 % collagenase (Wako Pure Chemicals) and then with 0.1 % trypsin (SIGMA), each for 20 min at 37°C. The DRGs were then dissociated by trituration with fire-polished Pasteur pipettes, and cells were plated onto glass coverslips coated with 0.01 % poly-L-lysine (SIGMA).

The dispersed DRG neurones were maintained in a humidified incubator containing 5 % CO_2 in air at 36°C in Dulbecco's modified Eagle medium supplemented with 10 % heat inactivated fetal bovine serum (GIBCO) , penicillin (100 IU/ml) and streptomycin (100 μg/ml). Cells under short-term culture (4 to 12 hr after plating) were used for experiments, unless otherwise specified. At this time in culture, neurite outgrowth was not observed.

Electrophysiology

Voltage-clamp recordings were performed using an Axopatch 200A amplifier (Axon Instruments, Inc.). Data were low-pass-filtered at 5 kHz with a four-pole Bessel filter and digitally sampled at 25-100 kHz. In some experiments, capacitive and leakage currents were subtracted digitally by the P-P/4 procedure (Ogata & Tatebayashi, 1993). Membrane currents were recorded using either the 'conventional' whole-cell patch-clamp technique (Hamill et al. 1981) or the nystatin-perforated patch technique (Horn & Marty, 1988). The standard pipette solution contained (in mM) ; 10 NaCl, 130 CsCl, 2.5 $MgCl_2$, 5 HEPES and 5 EGTA. The pH of the pipette solution was adjusted to 7.0 with CsOH. Osmolarity was adjusted to 290 mosmol/kg with glucose. In some experiments,

CsCl was totally replaced with an equimolar amount of CsF or Cs-salts of other several anions (see Fig. $7B_1$). For the internal pipette solution of nystatin-perforated patch recordings, a stock solution containing 10mg/ml nystatin (Wako Pure Chemicals) was prepared and added to the patch pipette solution to reach final concentration of 500 μg/ml. The DC resistance of patch electrodes was 0.8-1.5 MΩ for the conventional whole-cell patch and 2-3 MΩ for the nystatin-perforated patch, respectively.

The bath solution contained (in mM); 130 NaCl, 5 CsCl, 1.8 $CaCl_2$, 1 $MgCl_2$, 0.1 $CdCl_2$, 5 HEPES, and 25 Glucose. Ca^{2+} currents were completely blocked by 100 μm Cd^{2+} (Tatebayashi and Ogata, 1992). The pH of the bath solution was adjusted to 7.4 with NaOH. Osmolarity was adjusted to 290 mosmol/kg with glucose. The liquid junction potential between internal and external solutions was compensated for by adjusting the zero current potential to the liquid junction potential. Only cells showing an adequate voltage and space clamp were used (Ogata and Tatebayashi, 1993). Since the $Na_v1.9$ current was observed preferentially in small DRG neurones, all the experiments were performed on small DRG neurones less than 30 μm in diameter. Experiments were performed at room temperature (21-23°C) . Data are expressed as the mean ± S.E.M., and *n* represents the number of cells examined.

RESULTS

I_{NaN} recorded with F^- as an internal anion

Fig. 1 summarizes the Na^+ current mediated by $Na_V1.9$ (I_{NaN}) recorded from small DRG neurones of $Na_V1.8$-null mutant mice. The holding potential (V_h) negative to -120 mV was required to remove inactivation. The current could be activated at a test potential (V_t) as low as -90 mV. The time courses of activation and inactivation were extremely prolonged particularly at smaller depolarizing V_ts, thus producing a persistent Na^+ current (Fig. $1A_1$). I_{NaN} could be clearly separated from the TTX-sensitive (TTX-S)/fast Na^+ current due to its extremely slow kinetics (Fig. $1A_2$ and A_3). The peak amplitude of the current was extremely variable depending on the cell recorded (usually 1-10 nA, often exceeding 10 nA). The current-voltage curve was markedly extended to more negative voltages as compared with other known Na^+ currents (Fig. 1B). These fundamental properties of I_{NaN} are basically similar to those reported by Cummins et al. (1999). Since they used F^- as an internal anion, we also employed F^- in the above recordings. However, it is well known that F^- often gives rise to unusual effects on the channel kinetics (Breakwell et a. 1995). For instance, F^- in the patch pipette causes a hyperpolarizing shift of the steady-state inactivation (h_∞) (Vargas et al. 1999). Therefore, there may be a possibility that the unusual kinetics of I_{NaN} were due to F^-.

A family of I_{NaN}s in Fig. 2A was recorded intermittently within 10 min after rupture of patch membrane. Although the peak amplitudes evoked from V_h of -80 mV were relatively large in the initial stage (A_1), they became progressively smaller with time (A_2 and A_3). However, when V_h was changed to -120 mV, the peak amplitudes recovered to

a considerable extent (compare A_3 and A_4). It should be noted that the activation threshold was shifted to -90 mV (A_4) from -60 mV in the initial stage (A_1 and A_2). As shown in Fig. 2B, h_∞ curves measured 10-15 min after the first measurements unequivocally shifted to more negative potentials in all the cells examined. These results strongly suggest that F^- caused a hyperpolarizing shift of the voltage-dependence of the steady-state activation (m_∞) and h_∞.

I_{NaN} recorded with Cl^- as an internal anion

Fig. 3 summarizes I_{NaN} recorded with Cl^- as an internal anion. I_{NaN}s could be evoked even with a V_h of -60 mV (Fig. 3A). This finding indicates that the channel activity is retained without being inactivated even at -60 mV, when Cl^- was used as an internal anion. A family of I_{NaN}s was recorded intermittently within 10 min after rupture of patch membrane (Fig. 3B). The activation threshold was kept constant to -60 mV, even when V_h was shifted to more negative potentials (B_1 - B_4). Inactivation of channels by membrane depolarization proceeds more slowly when Cl^- was used (Fig. 3C). In addition, I_{NaN} was more resistant to depolarization than TTX-S/fast Na^+ current, when measured with Cl^- (Fig. 3D). With preceding conditioning pulses (V_{pre}) positive to -70 mV, the initial component reflecting TTX-S/fast Na^+ current was totally inactivated, whereas I_{NaN} remained unaffected. These results confirm that F^- but not Cl^- has caused a hyperpolarizing shift of the voltage-dependence of m_∞ and h_∞. In addition to these kinetic differences found between I_{NaN}s recorded with F^- and Cl^- internal anions, the amplitude of I_{NaN} recorded with Cl^- was generally much smaller than that recorded with

F^-. I_{NaN} of at most a few nA was commonly observed when Cl^- was used (Fig. 3), and such a huge I_{NaN} exceeding 10 nA as those seen with F- was never observed,

Activation and inactivation kinetics of I_{NaN}

Since the kinetics of I_{NaN} measured with F^- was shown to be distorted as shown above, we re-investigated the currents with Cl^- as an internal anion. The results shown in Fig. 4 are the typical examples of the 'normal' kinetics for I_{NaN} confirmed in a number of cells. A family of I_{NaN}s in response to various V_ts (Fig. 4A) shows that the current can be evoked at potentials positive to -60 mV. The maximal peak amplitude was obtained at -10 mV (Fig. 4B). In Fig. 4C, the m_∞ and h_∞ curves for I_{NaN} were compiled according to the methods described by Ogata & Tatebayashi (1993). The $V_{1/2}$ for m_∞ was -31.5 ± 1.4 mV (n = 4), and the $V_{1/2}$ for h_∞ was -42.3 ± 1.7 mV (n = 4). The $V_{1/2}$ for h_∞ is much positive than the values obtained for other Na^+ currents (Ogata et al. 1989; Ogata & Tatebayashi, 1990; Ogata et al. 1990). As a consequence, the two curves overlap at a wide range of voltage from -60 mV to -20 mV (shaded area in Fig. 4C).

Temporal changes of the functional expression of I_{NaN}

The functional expression of I_{NaN} was unstable either following acute isolation of cells from DRG or during culture. Fig. 5A summarizes the temporal change of the proportion of cells that expressed I_{NaN} following acute isolation. Although the majority of cells expressed I_{NaN} within 24 hours after dissociation, the percentage of cells expressing I_{NaN} declined with time, and most of the cells examined later than 48 hours after dissociation

no longer expressed detectable I_{NaN}. It seemed as if channels that mediate I_{NaN} fell away without being replenished with newly synthesized or recycled channels.

We also found that the functional expression of I_{NaN} can recover during culture (Fig. 5B). The percentage of cells expressing I_{NaN} initially declined as was shown in Fig. 5A. However, the percentage increased during culture in step with neural outgrowth or concurrent proliferation of non-neuronal cells (see the photomicrographs in Fig. 5B). The percentage of cells expressing I_{NaN} peaked when neural cells are surrounded with confluent non-neuronal cells (see the photograph for '7 days'). Neural cells having fully developed neurites but unaccompanied by non-neuronal cells (see the photograph for '12 days') again lost the current. Thus, it may be suggested that the co-expression of the non-neuronal cells is more important for the expression of the I_{NaN} than the outgrowth of neurites.

Comparison of two types of TTX-R Na^+ currents

Since we have used $Na_V1.8$ (SNS)-null mutant mice, another type of TTX-R Na^+ current (I_{SNS}) was absent throughout the experiments described above. In view of the striking differences in their kinetics, it might be useful to compare these two currents in the same neurone. Fig. $6A_1$ illustrates a family of heterogeneous Na^+ currents recorded from a naive mouse using F^- as an internal anion in the presence of TTX. Currents evoked by V_ts positive to the activation threshold for I_{SNS} (-40 mV, Ogata & Tatebayashi, 1993) in A_1 are shown in expanded time scale in A_2. Since the voltage-dependence of

m_∞ for I_{NaN} is markedly shifted to negative potentials by F^- (Fig. 2), the two components representing I_{NaN} and I_{SNS} could be separated. In addition, I_{SNS} could be evoked in isolation by changing V_h from -120 mV (A_1 and A_2) to -80 mV (A_3), since the voltage-dependence of h_∞ for I_{NaN} are also shifted in the hyperpolarizing direction by F^-.

When Cl^- was used as an internal anion, Na^+ currents evoked by V_ts between -60 mV and -40 mV represented a single component comprising I_{NaN}, since the activation threshold for I_{NaN} was about 20 mV more negative than the threshold for I_{SNS} (see Fig. 4). With more positive V_ts, the two components overlapped each other making the separation difficult. The two components could only be accidentally distinguished in the undesirable situation where the voltage clamp control was poor. For instance, in Fig. 6B, V_t to -30 mV evoked the Na^+ current apparently comprising two components. This was due to the fact that the faster and larger I_{SNS} escaped the voltage-clamp control whereas slower and smaller I_{NaN} remained controlled. Fig. 6C illustrates typical examples of the two TTX-R currents (C_1, I_{NaN} and C_2, I_{SNS}). The duration of I_{NaN} was more than 10 times longer than that of I_{SNS}.

'Kindling' of I_{NaN}

Fig. $7A_1$ shows the plot of the peak amplitude of I_{NaN} evoked intermittently by 2 Hz V_t using F^- as an internal anion. During recording, the peak amplitude started to increase and eventually reached up to more than 20 times the initial value, and then declined towards the original amplitude. Total duration of this spontaneous and explosive

increase-decrease of the peak amplitudes (referred to as the 'kindling' of I_{NaN}) took nearly 25 min. Current traces corresponding to the points indicated by numerals in A_1 are illustrated sequentially (A_2) or superimposed (A_3). The currents had essentially an identical time course as shown in A_4, indicating that the kindling of I_{NaN} was not due to a change in gating kinetics.

The kindling of I_{NaN} was not due to F^-, since the plots performed using several kinds of anions unequivocally showed similar change (Fig. 7B). However, both the increase of the amplitude and its duration were always much larger for F^- than for any other anions (note the amplitudes for F^- in Fig. 7B are shown with a reduced scale). The latency was variable depending on the cell examined as shown in Fig. $7B_2$. The very important point is that the amplitude of I_{NaN} measured before or after the kindling of I_{NaN} was very small irrespective of the anion used. The amplitude of I_{NaN} measured at the initial stage of recording with V_t to -30 mV using Cl^- as an internal anion was 263.2 ± 29.1 pA (n = 11).

Three sets of current traces in Fig. 7C were recorded in response to identical V_ts during the latent period (C_1), at the peak of the augmentation (C_2), and while the amplitude was decreasing (C_3). The three sets of currents had similar voltage-dependence, confirming that the gating kinetics *per se* remained unaffected during the kindling of I_{NaN}. To confirm whether this peculiar phenomenon is inherent to $Na_v1.9$, we examined the time courses of the peak amplitude for I_{SNS} and TTX-S/fast Na^+ current. The peak amplitude

of these Na^+ currents remained perfectly constant for more than 15 min in all the cells examined (n = 5 for each current; data, not illustrated).

I_{NaN} recorded under nystatin-perforated whole-cell patch-clamp

In contrast to the recordings with 'conventional' whole-cell patch-clamp, when the nystatin-perforated patch was applied, the peak amplitude of I_{NaN} remained constant throughout an extended period of recording (Fig. 8A). The amplitude of I_{NaN} evoked with V_t to -30 mV was 276.7 ± 56.6 pA (n = 6), much the same as that obtained at the initial stage of recording with conventional whole-cell patch. The current-voltage relationship for I_{NaN} measured with the nystatin-perforated patch showed a voltage-dependence identical to that for I_{NaN} measured with conventional whole-cell patch (Fig. 8B). $V_{1/2}$ and the slope factor of the h_∞ curves obtained with the nystatin-perforated patch was -42 mV and 12.3, respectively (Fig. 8C). Thus, I_{NaN} measured with the nystatin-perforated patch had the same kinetic properties as those measured with conventional whole-cell patch.

The preventive effect of internal ATP on the 'kindling' of I_{NaN}

On the assumption that the kindling of I_{NaN} observed with conventional whole-cell patch was due to washout of some important intracellular milieu, we attempted to record I_{NaN} with conventional whole-cell patch pipette supplemented with 2 mM ATP. Surprisingly, the kindling was not observed in any of 8 cells examined. Plots of the peak amplitude of I_{NaN} measured with supplemented intracellular ATP are illustrated in Fig. 9A. Sets of a

family of I_{NaN}s evoked at indicated periods after rupture of the patch membrane (Fig. 9B) confirm that the current-voltage relationship for I_{NaN} was not affected throughout the entire period of recording.

DISCUSSION

Shift of m_∞ and H_∞ by internal F^-

The Na^+ current mediated by $Na_V1.9$, I_{NaN}, has been identified by Commins et al. (1999) using the same mutant mice as those used in our study (Akopian et al. 1999). The results presented here add new information as to the unique electrophysiological properties of $Na_V1.9$. I_{NaN} originally reported (Cummins et al. 1999) had some peculiar properties, considering the common properties of the voltage-gated Na^+ channels, For instance, the activation threshold was shifted to an extremely negative potential (about –90mV). In addition, unless V_h was more negative than –120 mV, an appreciable amount of current was not evoked, indicating that the h_∞ curve was shifted to very negative potentials.

Our findings based on recordings using different internal anions elucidated that the above extraordinary kinetics for I_{NaN} had been due to F^- used as an internal anion. Namely, our results that the parameters, m_∞ and H_∞, for I_{NaN} observed with Cl^- as an internal anion were strikingly different from those observed with F^- demonstrate that the kinetic properties of I_{NaN} are strongly affected by internal F^-. The abnormal kinetic

behaviors induced by F^- may be attributed to miscellaneous actions of F^- on the cellular transduction system. For instance, F^- acts as an activator of G-proteins (Sternweis and Gilman, 1982; Yatani & Brown, 1991; Kuryshev et al. 1993), and the attenuation of Ca^{2+} current run-down by F^- in hippocampal neurones has been attributed to this action (Breakwell et al. 1995). Moreover, the hyperpolarizing shift of h_∞ for the hyperpolarization-activated current (I_h) has been shown to be due to reduction of cAMP-dependent protein kinase activity (Vargas et al. 1999).

$Na_V1.9$ as an 'inducible' Na^+ channel

The observation that the functional expression of I_{NaN} after acute isolation from DRG declined with time (Fig. 5A) might suggest that I_{NaN} might be dynamically regulated by trophic factors or a subtle environmental change for its survival. This notion is further supported by the observation that I_{NaN} recovered during culture in parallel with the growth of non-neuronal cells (Fig. 5B). In fact, it has been shown that glial-derived nerotrophic factor up-regulates expression of $Na_V1.9$ (Cummins et al. 2000). The mechanical disruption of nerve cells could result in a decreased supply of neurotrophic substances from surrounding non-neuronal cells such as Schwann cells, and non-neuronal cells that proliferate during culture could restore the decreased supply of neurotrophic substances. This may account for the loss of I_{NaN} following dissociation and its recovery during culture.

GDNF (glial cell line-derived neurotrophic factor) has roles as a potent survival factor

for certain classes of neurones and as a protective factor against nerve injury (Bennett et al. 1998; Fjell et al., 1999). It has also been shown that the small DRG neurones expressing $Na_V1.9$ are dependent on GDNF (Waxman et al. 1999; Fjell et al. 2000). In addition, GDNF actually up-regulates $Na_V1.9$ (Boucher et al. 2000). These findings strongly suggest that $Na_V1.9$ is regulated by GDNF. The regulation of $Na_V1.9$ could be exaggerated under pathological conditions. Moreover, neurotrophins such as GDNF appear to have opposing effects on different types of Na^+ channels, e.g., down-regulating $Na_V1.3$ (Boucher et al. 2000). Such a dynamic and subtype-specific regulation of 'inducible' Na^+ channels probably plays a key role in certain types of Na^+ channel disorders including neuropathic pain. The inducible property of $Na_V1.9$ may also give a clue to the understanding of how tissue-specific expressions of Na^+ channels are regulated to conform their appropriate deployment in various tissues.

$Na_V1.9$ as a 'kindling' Na^+ channel

Our results show that the conventional whole-cell patch-clamp does not afford I_{NaN} having a stable amplitude, due to the spontaneous and explosive augmentation ('kindling') of I_{NaN} (Fig. 7). The kindling of I_{NaN} was totally different from so-called 'run-down' often seen in some voltage-gated ion channels. There was no consistent control amplitude for the current, since the kindling of I_{NaN} occurred with a variable latency and often lasted for longer than 30 min. Due to rupture of the patch membrane, pipette solution washes out cytoplasmic milieu, and the intracellular environment may be impaired. Thus, it is possible that the kindling of I_{NaN} was induced by some unusual

situation following the rupture of patch membrane. This notion is supported by the finding that the kindling of I_{NaN} could be prevented by using the nystatin-perforated patch-clamp in stead of the conventional patch recording (Fig. 8).

Although the kindling of I_{NaN} was observed regardless of the anion species used as an internal anion, the phenomenon was exceptionally intense and prolonged when F^- was used (Fig. $7B_1$). In addition, ATP supplemented in the patch internal solution (Fig. 9) could prevent the kindling of I_{NaN}. These results might suggest that some unknown alteration in intracellular transduction system initiates the kindling of I_{NaN}. Since the latency for kindling of I_{NaN} was usually less than 10 min (Fig. $7B_1$), it is unlikely that the $Na_V1.9$ channel protein is newly synthesized following rupture of the membrane. Activation of the 'inactive' or 'sleeping' channels may be more relevant explanation for the kindling of I_{NaN}.

At present, the cellular events underlying the kindling of I_{NaN} remain unclear. The elucidation of its mechanistic basis will undoubtedly help to clarify a novel mechanism for channel regulation. In addition, the kindling as well as the inducible properties of $Na_V1.9$ may provide an additional insight into the plasticity of Na^+ channels, which precipitates pathological pain states (Baker & Wood, 2001). In pathological states, inactive or 'silent' $Na_v1.9$ channels could be kindled by some unknown mechanism, whereas functional expression of $Na_v1.9$ is strictly controlled in normal condition, We are currently studying effects of various agents, which affect intracellular transduction

precipitates pathological pain states (Baker & Wood, 2001). In pathological states, inactive or 'silent' $Na_v1.9$ channels could be kindled by some unknown mechanism, whereas functional expression of $Na_v1.9$ is strictly controlled in normal condition, We are currently studying effects of various agents, which affect intracellular transduction system, on the kindling of I_{NaN}.

Recently, Blum et al. (2002) reported surprizing data that brain-derived neurotrophic factor (BDNF) induces a rapid membrane depolarization through an opening of $Na_V1.9$ in hippocampal neurones. Although the detailed molecular mechanism involved in this neurotrophin-evoked activation of $Na_V1.9$ remains unclear, there may be a possibility that the inducible and kindling properties of $Na_V1.9$ demonstrated in our study may share a common mechanistic basis with the neurotrophin-evoked activation of $Na_V1.9$. In this respect, it is tempting to examine whether BDNF or GDNF causes a rapid opening of the $Na_V1.9$ in DRG.

Distinct functional roles of the two types of TTX-R Na^+ channels

The two isoforms of TTX-R Na^+ channels, $Na_V1.8$ and $Na_V1.9$, are thought to have specialized roles in pain sensation (Waxman et al. 1999; Baker & Wood, 2001). An important question is whether these two populations of TTX-R Na^+ channels have distinct functional roles. Although it has been generally accepted that the conducting axonal action potentials are sensitive to TTX, evidence has been accumulating that nociceptive signals are rather dependent on TTX-R propagating action potentials in C-

nociceptors and transduced to action potentials. Recent two forms of studies attempting this direct approach (Brock et al. 1998; Strassman & Raymond, 1999) demonstrated that TTX-R but not TTX-S Na^+ channels contribute to the transduction of the nociceptive stimuli to conducting spikes at nerve terminals.

Nystatin-perforated patch-clamp recordings disclosed that I_{NaN} is an extremely small current less than 500 pA (Fig. $8B_1$), and this may reflect the 'normal' form of I_{NaN}, since I_{NaN} recorded during the latent period preceding to the kindling (Fig. $8B_1$) or I_{NaN} recorded with internal ATP (Fig. 9A) had similar small peak amplitudes. The possibility that the current is small due to subcellular distribution of $Na_V1.9$ limited to axons or nerve terminals may be excluded, since such a localized expression of $Na_V1.9$ within the neurone has not been demonstrated in immunohistochemical studies (Waxman et al. 2000). Thus, I_{NaN} in a 'normal' situation appears to be too small to carry an action potential. In contrast, another TTX-R Na^+ current, I_{SNS}, can mediate an action potential upstroke (Elliott & Elliott, 1993; Ogata & Tatebayashi, 1993). Thus, the TTX-R spikes generating at nerve terminals (Brock et al. 1998; Strassman & Raymond, 1999) may be mainly mediated by $Na_V1.8$ rather than $Na_V1.9$, although the possibility remains that $Na_V1.9$ may also directly contribute to spike generation when kindled in some abnormal situation.

$Na_V1.9$ as a subthreshold and 'background' Na^+ channel

There were several remarkable differences between I_{NaN} and other Na^+ currents. For

instance, I_{NaN} had an activation threshold of about -60 mV and a persistent time course, whereas the TTX-sensitive/fast Na^+ current and I_{SNS} had a threshold of about -40 mV and relatively fast gating kinetics. Na_V1 isoforms currently comprise nine highly homologous clones (Goldin, 2001). Although the functional role of Na_V1 isoforms is primarily to form an action potential upstroke in excitable cells, our results suggest that $Na_V1.9$ can also influence subthreshold electrical activity through a persistent Na^+ current. A similar role has also been implicated for persistent Na^+ currents found in a variety of tissues (Dubois & Bergman, 1975; Schwindt & Crill, 1977; French et al. 1990; Saint et al. 1992; Alzheimer et al. 1993; Stys et al. 1993; Chandler et al. 1994; Baker & Bostock, 1997; Kay et al. 1998). However, most of them are sensitive to TTX, suggesting that $Na_V1.9$ may not be involved in these known persistent Na^+ currents. Available data suggest that these TTX-S persistent Na^+ currents are possibly mediated by $Na_V1.6$ (Baker & Bostock, 1997; De Miera et al. 1997; Caldwell et al. 2000).

Even the transient type of Na^+ currents could give rise to a persistent Na^+ current through overlapping activation-inactivation kinetics (a window current) or a wide repertoire of gating mode ("mode switching"). However, in the case of I_{NaN}, the persistent nature of the current was primarily due to its slow activation and inactivation kinetics distinct from the transient Na^+ channels. I_{NaN} may play pivotal roles in regulating repetitive firing, amplifying subthreshold depolarizations, and producing after-depolarizations and plateau potentials. I_{NaN} may also be involved in disorders of neurones and neurites. Unlike transient Na^+ currents that are immediately inactivated

following membrane depolarization, persistent Na^+ currents continue to be activated during prolonged membrane depolarization. The resultant increase in $[Na^+]_i$ through persistent Na^+ influx, coupled with reverse operation of the Na^+-Ca^{2+} exchanger, may cause a damaging increase of $[Ca^{2+}]_i$ (Stys et al. 1992).

REFERENCES

AKOPIAN, A. N., SIVILOTTI, L. & WOOD, J. N. (1996). A tetrodotoxin-resistant sodium channel expressed by sensory neurons. *Nature* **379**, 257-262.

AKOPIAN, A. N., SOUSLOVA, V., ENGLAND, S., OKUSE, K., OGATA, N., URE, J., SMITH, A., KERR, B. J., MCMAHON, S. B., BOYCE, H., HILL, R., STANFA, L. C., DICKERSON, A. H. & WOOD. J. N. (1999). The tetrodotoxin-resistant sodium channel SNS has a specialized function in pain pathways. *Nature Neuroscience* **2**, 541-548.

ALZHEIMER, C., SCHWINDT, P. C. & CRILL, W. E. (1993). Modal gating of Na^+ channels as a mechanism of persistent Na^+ current in pyramidal neurons from rat and cat sensorimotor cortex. *Journal of Neuroscience* **13**, 660-673.

BAKER, M. D. & BOSTOCK, H. (1997). Low-threshold, persistent sodium current in rat large dorsal root ganglion neurons in culture. *Journal of Neurophysiology* **77**, 1503-1513.

BAKER, M. D. & WOOD, J.N. (2001). Involvement of Na^+ channels in pain pathways. *Trends in Pharmacological Sciences* **22**, 27-31.

BENNETT, D. L. H., MICHAEL, G. J., RAMACHANDRAN, N., MUNSON, J. B., AVERILL, S., YAN, Q., MCMAHON, S. B. & PRIESTLEY, J. V. (1998). A distinct subgroup of small DRG cells express GDNF receptor components and GDNF is protective for these neurons after nerve injury. *Journal of Neuroscience* **18**, 3059-3072.

BLUM, R., KAFITZ, K. W. & KONNERTH, A. (2002). Neurotrophin-evoked depolarization requires the sodium channel $Na_V1.9$. *Nature* **419**, 687-693.

BOUCHER, T. J., OKUSE, K., BENNETT, D. L., MUNSON, J. B. & WOOD, N. (2000). Potent analgesic effects of GDNF in neuropathic pain states. *Science* 290, 124-127.

BREAKWELL, N. A., BEHNISCH, T., PUBLICOVER, S. J. & REYMANN, K. G. (1995). Attenuation of high-voltage-activated Ca^{2+} current run-down in rat hippocampal CA1 pyramidal cells by NaF. Experimental Brain Research **106**, 505-508.

BROCK, J. A., MCLACHLAN, E. M. & BELMONE, C. (1998). Tetrodotoxin-resistant impulses in single nociceptor nerve terminals in guinea-pig cornea. *Journal of Physiology* **512**, 211-217.

CALDWELL, J. H., SCHALLER, K. L., LASHER, R. S., PELES, E. & LEVINSON, S. R. (2000). Sodium channel Na(v)1.6 is localized at nodes of Ranvier, dendrites, and synapses. *Proceedings of the National Academy of Sciences of the USA* **97**, 5616-5620.

CHANDLER, S. H., HSAIO, C. F., INOUE, T. & GOLDBERG, L. J. (1994). Electrophysiological properties of guinea pig trigeminal motoneurons recorded in vitro. *Journal of Neurophysiology* **71**, 129-145.

CUMMINS, T. R., BLACK, J. A., DIB-HAJJ, S. D. & WAXMAN, S. G. (2000). Glial-derived neurotrophic factor upregulates expression of functional SNS and NaN sodium channels and their currents in axtomized dorsal root ganglion neurons.

Journal of Neuroscience **20**, 8754-8761.

CUMMINS, T. R., DIB-HAJJ, S. D., BLACK, J. A., AKOPIAN, A. N., WOOD, J. N. & WAXMAN, S. G. (1999). A novel persistent tetrodotoxin-resistant sodium current in sns-null and wild-type small primary sensory neurons. *Journal of Neuroscience* **19**, 1-6.

DE MIERA, E. V. S., RUDY, B., SUGIMORI, M. & LLINAS, R. (1997). Molecular characterization of the sodium channel subunits expressed in mammalian cerebellar Purkinje cells. *Proceedings of the National Academy of Sciences of the USA* **94**, 7059-7064.

DIB-HAJJ, S., BLACK, J. A., CUMMINS, T. R. & WAXMAN, S. G. (2002). NaN/$Na_V1.9$: a sodium channel with unique properties. *Trends in Neurosciences* **25**, 253-259.

DIB-HAJJ, S. D., TYRRELL, L., BLACK, J. A. & WAXMAN, S. G. (1998). NaN, a novel voltage-gated Na channel is expressed preferentially in peripheral sensory neurons and down-regulated after axotomy. *Proceedings of the National Academy of Sciences of the USA* **95**, 8963-8968.

DUBOIS, J. M. & BERGMAN, C. (1975). Late sodium current in the node of Ranvier. *Pflügers Archiv* **357**, 145-148.

ELLIOTT, A. A. & ELLIOTT, J. R. (1993). Characterization of TTX-sensitive and TTX-resistant sodium currents in small cells from adult rat dorsal root ganglia. *Journal of Physiology* **463**, 39-56.

FJELL, J., CUMMINS, T. R., DIB-HAJJ, S. D., FREID, K., BLACK, J. A. &

WAXMAN, S. G. (1999). Differential role of GDNF and NGF in the maintenance of two TTX-resistant sodium channels in adult DRG neurons. *Molecular Brain Research* **67**, 267-282.

FJELL, J., HJELMASTRCÖM, P., MILENKOVIC, M., AGLIECO, F., TYRRELL, L., ., DIB-HAJJ, S. D., WAXMAN, S. G. & BLACK, J. A. (2000). Localization of the tetrodotoxin-resistant sodium channel NaN in nociceptors. *Molecular Neuroscience* **11**, 199-202.

FRENCH, C. R., SAH, P., BUCKETT, K. J. & GAGE, P. W. (1990). A voltage-dependent persistent sodium current in mammalian hippocampal neurons. *Journal of General Physiology* **95**, 1139-1157.

FUJIKAWA, S., MOTOMURA, H. & OGATA, N. (1997). $GABA_B$-mediated upregulation of the high-voltage-activated Ca^{2+} channels in rat dorsal root ganglia. *Pflügers Archiv* **434**, 84-90.

GOLD, M. S., REICHLING, D. B., SHUSTER, M. J. & LEVINE, J. D. (1996). Hyperalgesic agents increase a tetrodotoxin-resistant Na+ current in nociceptors. *Proceedings of the National Academy of Sciences of the USA* **93**, 1108-1112.

GOLDIN, A.L. (2001). Resurgence of sodium channel research. *Annual Review of Physiology* **63**, 871-894.

GROßKREUTZ, J., QUASTHOFF, S., KUHN, M. & GRAFE, P. (1996) Capsaicin blocks tetrodotoxin-resistant sodium potentials and calcium potentials in unmyelinated C fibers of biopsied human sural nerve in vitro. *Neuroscience Letters* **208**, 49-52.

HAMILL, O. P., MARTY, A., NEHER, E., SAKMANN, B. & SIGWORTH, F. J. (1981). Improved patch-clamp techniques for high-resolution current recording from cells and cell-free membrane patches. *Pflügers Archiv* **391**, 85-100.

HORN, R. & MARTY, A. (1988). Muscarinic activation of ionic currents measured by a new whole-cell recording method. *Journal of General Physiology* **92**, 145-159.

KAY, A. R., SUGIMORI, M. & LLINAS, R. (1998). Kinetic and stochastic properties of a persistent sodium current in mature guinea pig cerebellar Purkinje cells. *Journal of Neurophysiology* **80**, 1167-1179.

KURYSHEV, Y. A., MAUMOV, A. P., AVDONIN, P. V. & MOZHAYEVA, G. N. (1993). Evidence for involvement of a GTP-binding protein in activation of Ca^{2+} influx by epidermal growth factor in A431 cells: effects of fluoride and bacterial toxins. *Cellular Signalling* 5, 555-564.

LAI, J., HUNTER, J. C., OSSIPOV, M. H. & PORRECA, F. (2000). Blockade of neuropathic pain by antisense targeting of tetrodotoxin-resistant sodium channels in sensory neurons. *Methods in Enzymology* **314**, 201-203.

LAIRD, J. M. A., SOUSLAVA, V., WOOD, J. N. & CERVERO, F. (2002). Deficits in visceral pain and referred hyperalgesia in $Na_V1.8$ (SNS/PN3)-null mice. *Journal of Neuroscience* **22**, 8352-8356.

OGATA, N., NISHIMURA, M. & NARAHASHI, T. (1989). Kinetics of chlorpromazine block of sodium channels in single guinea pig cardiac myocytes. *Journal of Pharmacology and Experimental Thrapeutics* **248**, 605-613.

OGATA, N. & TATEBAYASHI, H. (1990). Sodium current kinetics in freshly isolated

neostriatal neurones of the adult guinea pig. *Pflügers Archiv* **416**, 594-603.

OGATA, N. & TATEBAYASHI, H. (1993). Kinetic analysis of two types of Na^+ channels in rat dorsal root ganglia. *Journal of Physiology* **466**, 9-37.

OGATA, N., Yoshii, M. & Narahashi, T. (1990). Differential block of sodium and calcium channels by chlorpromazine in mouse neuroblastoma cells. *Journal of Physiology* **420**, 165-183.

SAINT, D. A., JU., Y-K & GAGE, P. W. (1992). A persistent sodium current in rat ventricular myocytes. *Journal of Physiology* **453**, 219-231.

SATIN, J., KYLE, J. W., CHEN, M., ROGART, R. B. & FOZZARD, H. A. (1992). The cloned cardiac Na channel alpha-subunit expressed in Xenopus oocytes show gating and blocking properties of native channels. *Journal of Membrane Biology* **130**, 11-22.

STERNWEIS, P. C. & GILMAN, A. G. (1982). Aluminum: a requirement for activation of the regulatory component of adenylate cyclase by fluoride. *Proceedings of the National Academy of Sciences of the USA* **79**, 4888-4891.

STRASSMAN, A. M. & RAYMOND, S. A. (1999). Electrophysiological evidence for tetrodotoxin-resistant sodium channels in slowly conducting dural sensory fibers. *Journal of Neurophysiology* **81**, 413-424.

STYS, P. K., SONTHEIMER, H., RANSOM, B. R. & WAXMAN, S. G. (1993). Noninactivating, tetrodotoxin-sensitive Na^+ conductance in rat optic nerve axons. *Proceedings of the National Academy of Sciences of the USA* **90**, 6976-6980.

STYS, P. K., WAXMAN, S. G. & RANSOM, B. R. (1992). Ionic mechanisms of anoxic

injury in mammalian CNS white matter: role of Na^+ channels and Na^+-Ca^{2+} exchanger. *Journal of Neuroscience* **12**, 430-439.

TANAKA, M., CUMMINS, T. R., ISHIKAWA, K., DIB-HAJJ, S. D., BLACK, J. A. & WAXMAN, S.G. (1998). SNS Na^+ channel expression increases in dorsal root ganglion neurons in the carrageenan inflammatory pain model. *Neuroreport* **9**, 967-972.

Tatebayashi, H. & Ogata, N., (1992). Kinetic analysis of the GABAB-mediated inhibition of the high-threshold Ca2+ current in cultured rat sensory neurones. Journal of Physiology, 447, 391-307.

VARGAS, G., YEH, T. J., BLUMENTHAL, D. K. & LUCERO, M. T. (1999). Common components of patch-clamp internal recording solutions can significantly affect protein kinase A activity. *Brain Research* **828**, 169-173.

YATANI, A. & BROWN, A. M. (1991). Mechanism of fluoride activation of G protein-gated muscarinic atrial K^+ channels. *Journal of Biological Chemistry* **266**, 22872-22877.

WAXMAN, S. G., DIB-HAJJ, S., CUMMINS, T. R. & BLACK, J. A. (1999). Sodium channels and pain. *Proceedings of the National Academy of Sciences of the USA* **96**, 7635-7639.

WAXMAN, S. G., DIB-HAJJ, S. D., CUMMINS, T. R. & BLACK, J. A. (2000). Sodium channels and their genes : dynamic expression in the normal nervous system, dysregulation in the disease states. *Brain Research* **886**. 5-14.

Figure legends

Figure 1. Na^+ currents mediated by $Na_V1.9$ (I_{NaN}) in isolated dorsal root ganglion (DRG) neurones of $Na_V1.8$-null mutant mice

A, Na^+ currents evoked by a 200 ms test pulse (V_t) from a holding potential (V_h) of –120 mV. A_1 illustrates a family of superimposed I_{NaN}s evoked by V_t indicated by the voltage attached to each trace. A_2 I_{NaN} evoked by V_t to –30 mV is shown separately to indicate two components of the current. Open and filled arrows indicate tetrodotoxin-sensitive (TTX-S)/fast (truncated) and $Na_V1.9$ components, respectively. A_3, the protocol in A_1 was repeated in the presence of 0.1 μM TTX. B, the current-voltage curve compiled from traces in A_3. In this figure, F^- was used as an internal anion (see Methods). Since the majority of currents were recorded with Cl^- as an internal anion in the present study, only traces recorded with F^- were specified in subsequent figures. Similarly, since the majority of currents were recorded in $Na_V1.8$-null mutant mice in the presence of 0.1 μM TTX, only traces recorded in naive mice or in the absence of TTX were specified.

Figure 2. Kinetic effects of F^- on I_{NaN}

A, four sets of I_{NaN}s were recorded intermittently within 10 min after rupture of patch membrane. TTX was not included in the external solution. V_h was –80 mV for A_1-A_3 and -120 mV for A_4. Voltage attached to each trace indicates V_t. The TTX-sensitive/fast Na^+ component was truncated in A_4. B, steady-state inactivation (h_∞) curves measured

with F^- as an internal anion. Inset diagram illustrates the pulse protocol. Two identical step pulses to –30 mV for 200 ms were applied 10 s prior (V_c) and immediately subsequent (V_t) to the conditioning prepulse (V_{pre}) from V_h of –80 mV. The pulse protocol was repeated twice in the same neurone with an interval of 10-15 min. The peak amplitude of the current evoked by V_t (I_t) was divided by the peak amplitude obtained with V_c (I_c), and the ratio was plotted against V_{pre}. The solid and broken lines represent first and second measurements, respectively.

Figure 3. Gating kinetics for I_{NaN} measured by Cl^- as an internal anion

A, a family of superimposed I_{NaN}s evoked from V_h of –60 mV. B, four sets of I_{NaN}s were recorded intermittently within 10 min after rupture of patch membrane. Each family of superimposed current traces was evoked from different V_h (A_1, -60 mV; A_2, -80 mV; A_3, -100 mV, A_4, -120 mV). C, time course of inactivation was assessed by the protocol shown in the inset. Two identical step pulses to –30 mV for 200 ms were applied 10 s prior (V_c) and immediately subsequent (V_t) to the conditioning prepulse (V_{pre}) to –50 mV from V_h of –120 mV. The duration of V_{pre} (ΔT) was progressively increased upto 4 s. Open circles, Cl^--internal anion; closed circles, F^--internal anion. D, V_c and V_t were applied 10 s prior and immediately subsequent to V_{pre} from V_h of –80 mV. TTX was not included in the external solution. The duration of V_{pre} was fixed to 2 s and the voltage was changed from -100 mV to -40 mV.

Figure 4. Typical kinetics of I_{NaN} measured with Cl^- as an internal anion

A, a family of superimposed I_{NaN}s. B, the current-voltage curve compiled from traces in A. C, the steady-state activation (m_∞) and inactivation (h_∞) curves for I_{NaN}. The procedure for making m_∞ curve was described in Ogata and Tatebayashi (1993). The pulse protocol for h_∞ curve is shown in Fig. 3D. $V_{1/2}$ and slope factor (S.F.): -31 mV and 9.2 for m_∞; -42 mV and 7.4 for h_∞.

Figure 5. Functional expression of I_{NaN} after isolation and during culture

A, a proportion of cells that manifested I_{NaN} to the total number of cells tested was counted at various periods after isolation of cells from DRG (A) and during culture (B). Each column was computed from more than 50 cells tested. Photographs in B depict phase-contrast microscopic view of culture at periods indicated in abscissa.

Figure 6. Comparison of two types of TTX-R Na^+ currents

A, heterogeneous Na^+ currents recorded from a small DRG neurone of the naive mouse. F^- was used as an internal anion. A_1, a family of Na^+ currents evoked by different V_ts. A_2, some of the currents shown in A_1 are shown separately to indicate two distinct components of the current. Open or filled arrows indicate the component mediated by $Na_V1.8$ or $Na_V1.9$, respectively. Positive shift of V_h from –120 mV (A_1 and A_2) to –80 mV (A_3) isolated the component mediated by $Na_V1.8$ due to inactivation of the component mediated by $Na_V1.9$. B, heterogeneous Na^+ currents recorded from the small DRG neurone of naive mouse using Cl^- as an internal anion. In this particular cell, two components representing distinct TTX-resistant Na^+ currents can be clearly

distinguished at V_t of –30 mV (explanation, see text). C, typical examples of the two types of TTX-R Na^+ currents are shown separately. C_1, I_{NaN} (in the absence of TTX); C_2, Na^+ currents mediated by $Na_V1.8$. The arrow in C_1 indicates TTX-S/fast Na^+ current that can be easily distinguished from I_{NaN}. C_2 was recorded from a cultured DRG neurone of the naive mouse that was devoid of I_{NaN}. The left traces in C_2 was drawn with the same time scale as in C_1 for comparison.

Figure 7. 'Kindling' of I_{NaN} during whole-cell recording

A_1, I_{NaN} was intermittently evoked by 2 Hz V_t to –50 mV from V_h of –120 mV, and its peak amplitude was plotted as a function of time. Traces indicated by numbers (1-18) in A_1 were shown sequentially (A_2), superimposed (A_3), and normalized to the largest current (A_4). A_1 - A_4 were all recorded using F^- as an internal anion. B, peak amplitudes of I_{NaN} plotted as in A_1. B_1, several kinds of anions were used for the internal solution. The amplitudes for F^- were reduced to a quarter. B_2, two examples of plots having similar degree of augmentation of the peak amplitude but different latent periods. C, a family of I_{NaN}s recorded 1, 9 and 11 min after rupture of patch membrane. V_t, from –60 mV to 0 mV. V_h, -80 mV.

Figure 8. I_{NaN} recorded under nystatin-perforated whole-cell patch-clamp

A, peak amplitudes of I_{NaN} were plotted as in Fig. $7A_1$. Symbols, measurements with nystatin-perforated whole-cell patch-clamp. An example made with conventional whole-cell patch-clamp is also illustrated for reference (broken line). Inset traces

illustrate the I_{NaN} recorded using nystatin-perforated patch at 1, 4, 9, and 16 min after perforation of the patch membrane. B_1, a family of I_{NaN}s evoked by different V_ts using nystatin-perforated patch-clamp. B_2, the current-voltage curve compiled from traces in B_1. C, h_∞ curve measured using nystatin-perforated patch-clamp. For pulse protocol, see Fig. 2B. $V_{1/2}$ and slope factor (S.F.) were -42 mV and 12.3, respectively.

Figure 9. The preventive effect of internal ATP on the spontaneous augmentation of I_{NaN}

A, peak amplitudes of I_{NaN} measured with conventional whole-cell patch-clamp were plotted as in Fig. $7A_1$. Filled symbols, 2 mM Mg^{2+}-ATP (Sigma) was added to internal solution of the patch electrode. Open circle, Mg^{2+}-ATP was not added. B, a family of I_{NaN}s recorded intermittently at indicated periods after rupture of patch membrane. Patch pipette contained 2 mM Mg^{2+}-ATP.

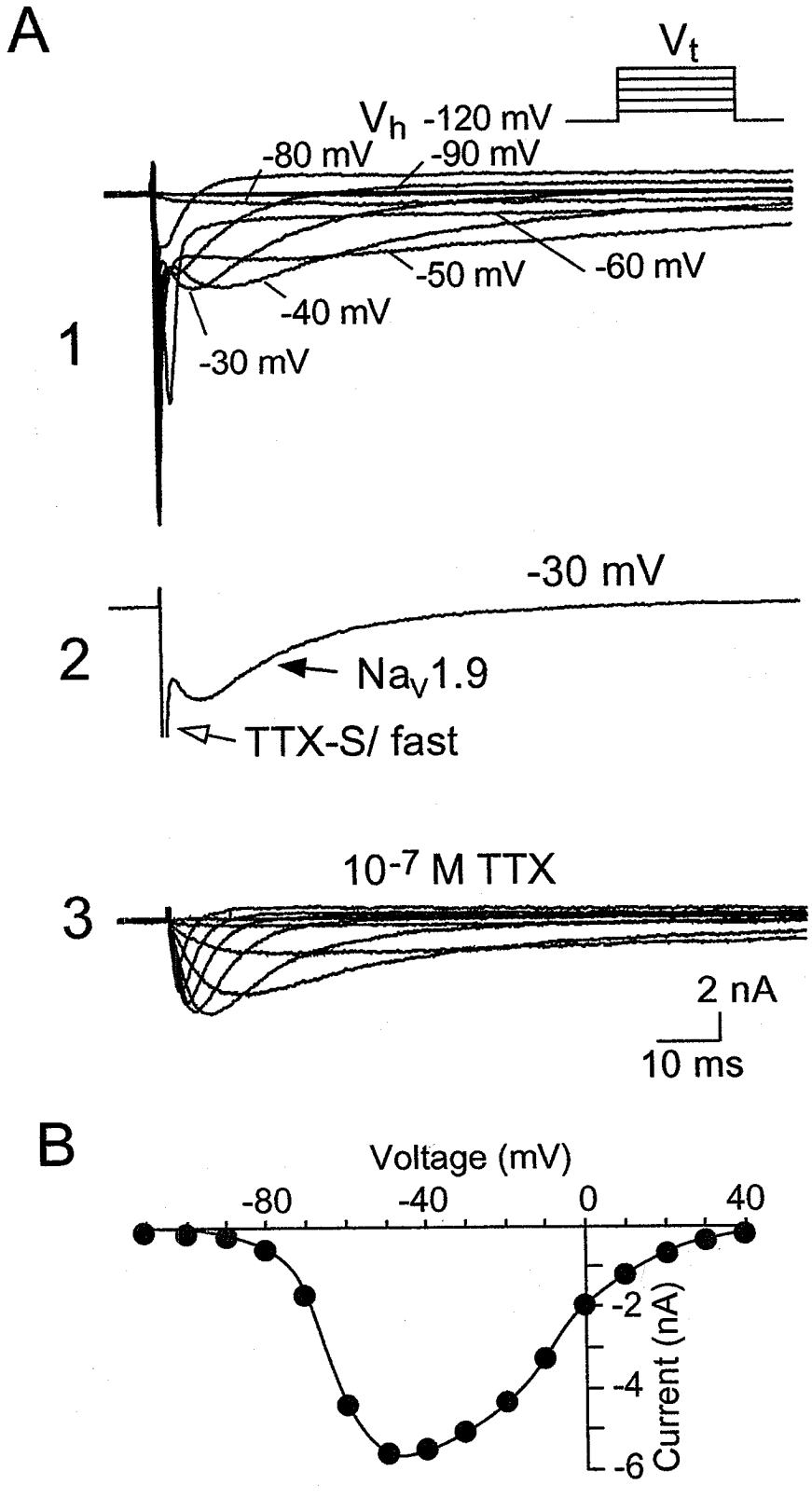
A
V_t
V_h -120 mV
-80 mV
-90 mV
-50 mV
-60 mV
-40 mV
-30 mV
1
-30 mV
2
$Na_V1.9$
TTX-S/ fast
10^{-7} M TTX
3
2 nA
10 ms
B
Voltage (mV)
-80
-40
0
40
-2
-4
-6
Current (nA)

Fig. 1

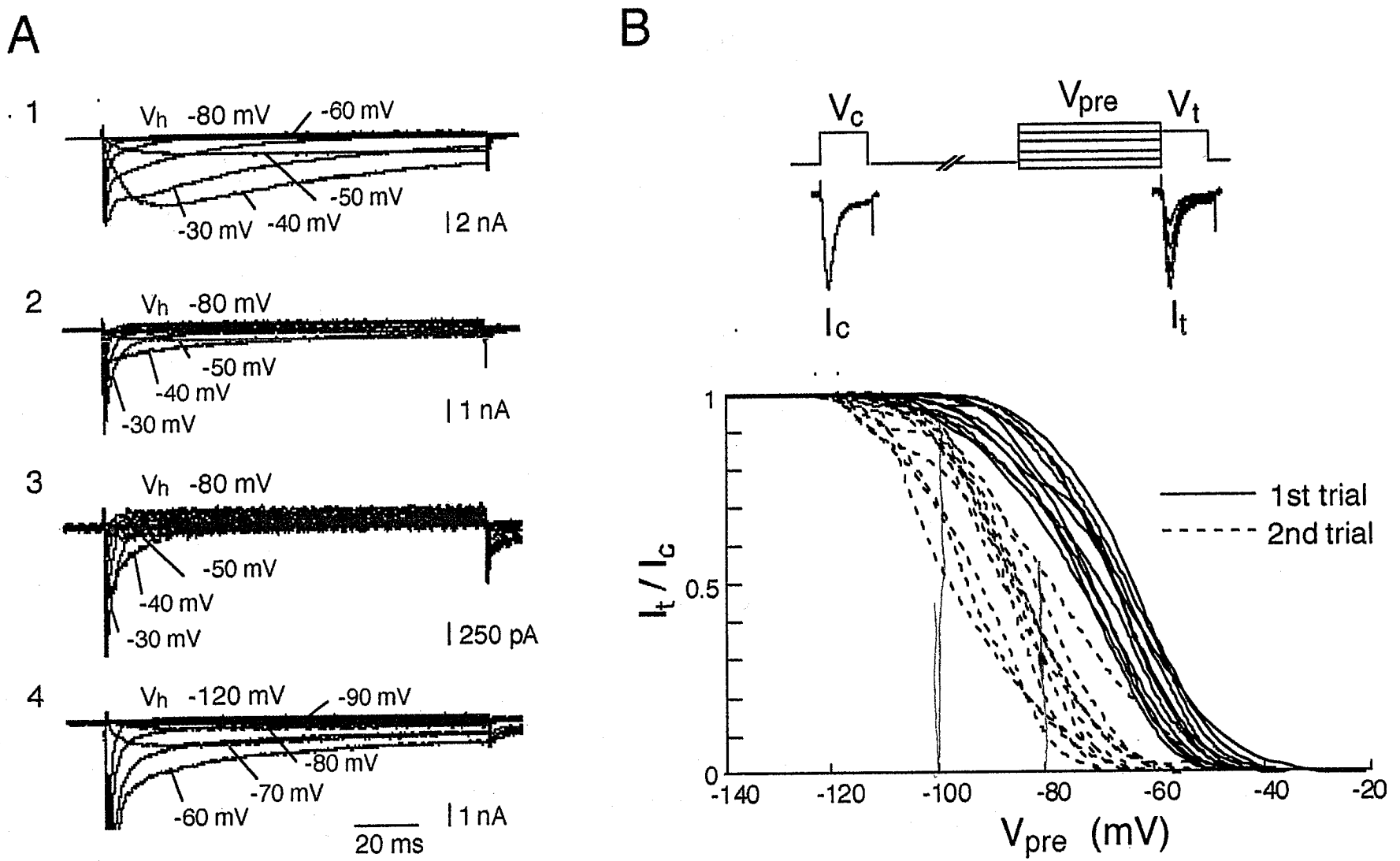
A
1
Vh -80 mV
-60 mV
-50 mV
-30 mV
-40 mV
2 nA
2
Vh -80 mV
-50 mV
-40 mV
-30 mV
1 nA
3
Vh -80 mV
-50 mV
-40 mV
-30 mV
250 pA
4
Vh -120 mV
-90 mV
-80 mV
-70 mV
-60 mV
1 nA
20 ms
B
Vc
Vpre
Vt
Ic
It
It / Ic
1
0.5
0
-140
-120
-100
-80
-60
-40
-20
Vpre (mV)
1st trial
2nd trial

Fig. 2

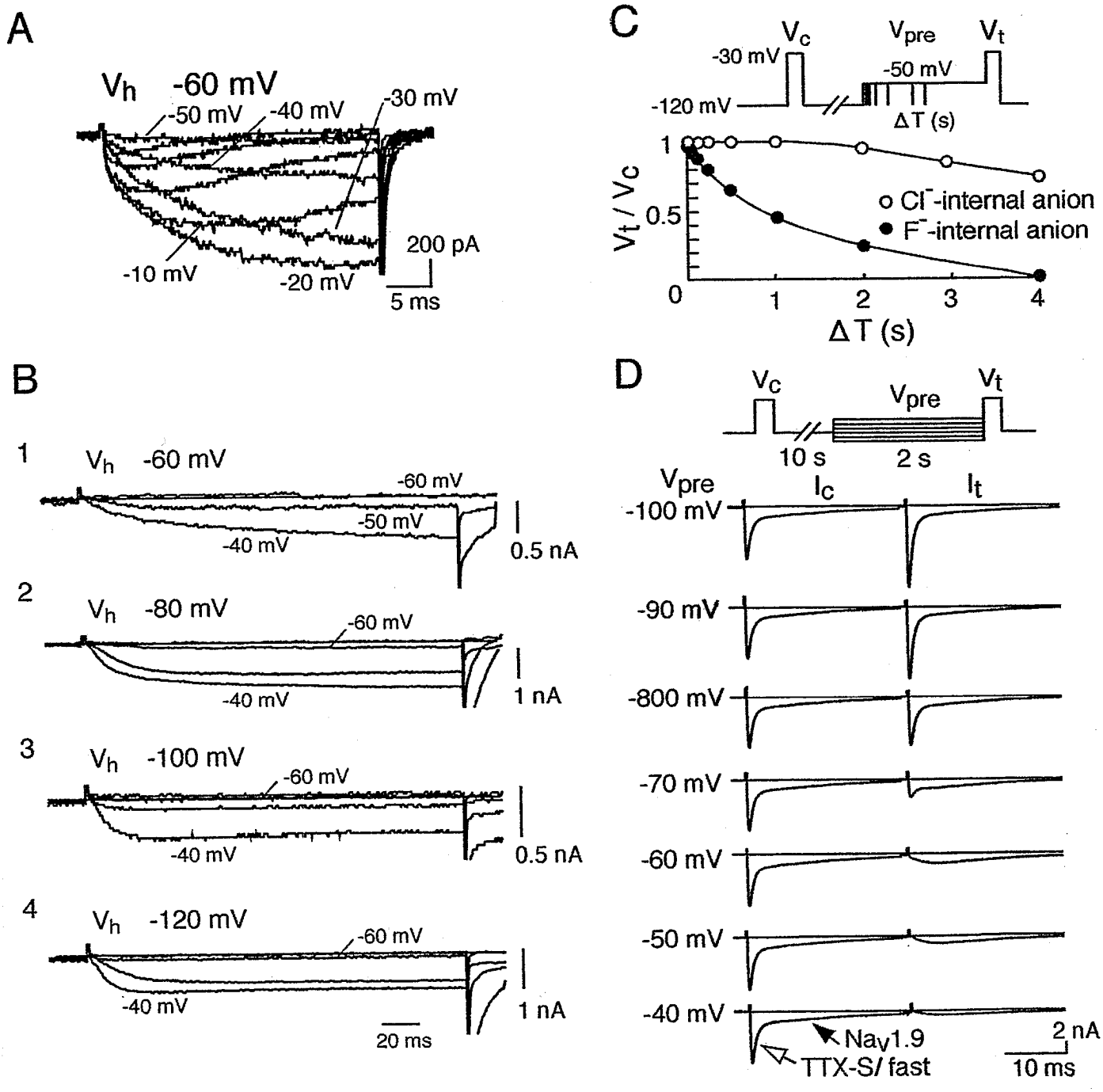
A
Vh -60 mV
-50 mV
-40 mV
-30 mV
-10 mV
-20 mV
200 pA
5 ms
B
1
Vh -60 mV
-60 mV
-50 mV
-40 mV
0.5 nA
2
Vh -80 mV
-60 mV
-40 mV
1 nA
3
Vh -100 mV
-60 mV
-40 mV
0.5 nA
4
Vh -120 mV
-60 mV
-40 mV
20 ms
1 nA
C
Vc
Vpre
Vt
-30 mV
-50 mV
-120 mV
ΔT (s)
Vt / Vc
1
0.5
0
1
2
3
4
ΔT (s)
Cl⁻-internal anion
F⁻-internal anion
D
Vc
Vpre
Vt
10 s
2 s
Vpre
Ic
It
-100 mV
-90 mV
-800 mV
-70 mV
-60 mV
-50 mV
-40 mV
NaV1.9
TTX-S/ fast
2 nA
10 ms

Fig. 3

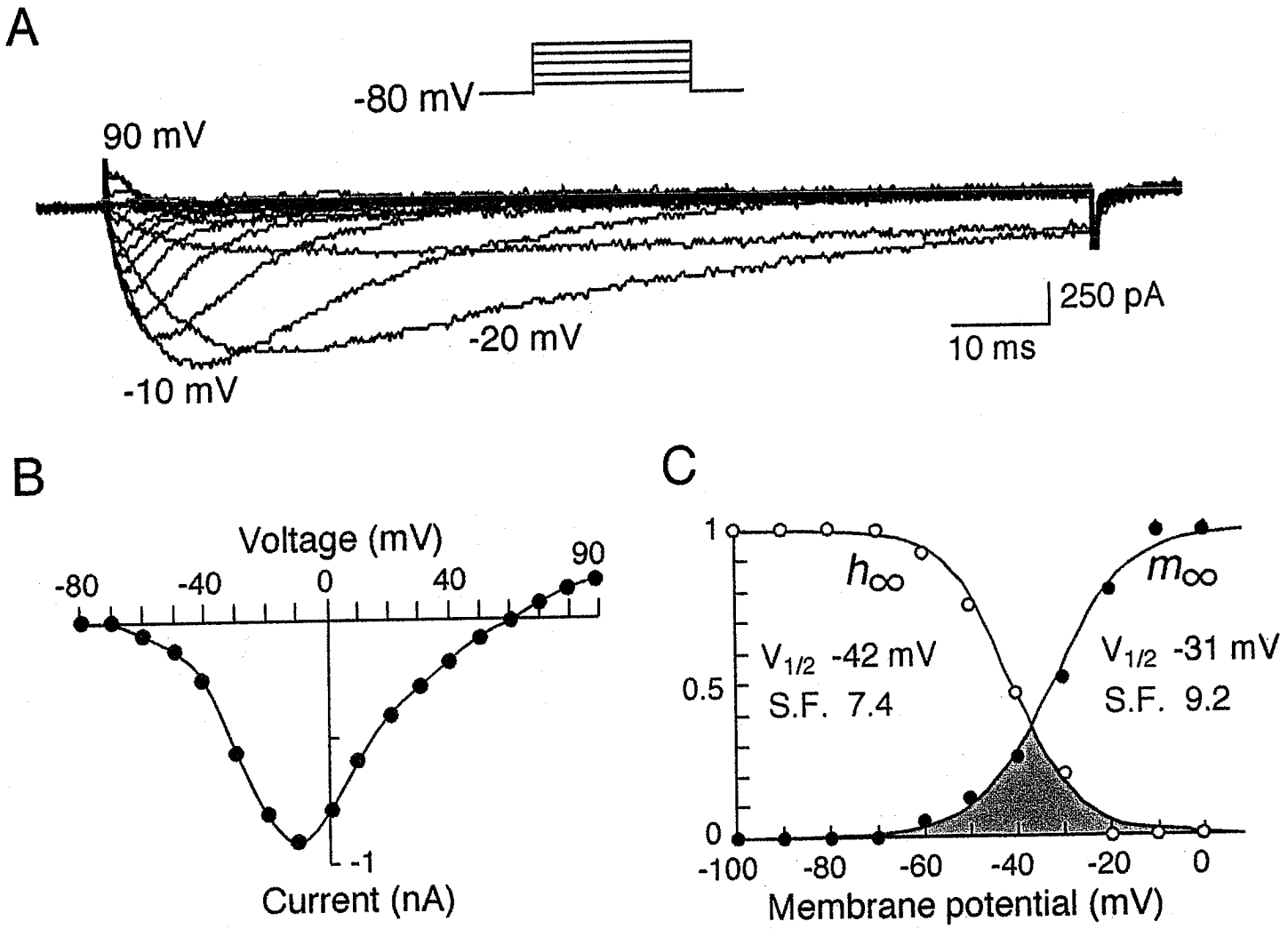
A
-80 mV
90 mV
250 pA
10 ms
-20 mV
-10 mV
B
Voltage (mV)
-80
-40
0
40
90
-1
Current (nA)
C
1
0.5
0
h_∞
m_∞
$V_{1/2}$ -42 mV
S.F. 7.4
$V_{1/2}$ -31 mV
S.F. 9.2
-100
-80
-60
-40
-20
0
Membrane potential (mV)

Fig. 4

A

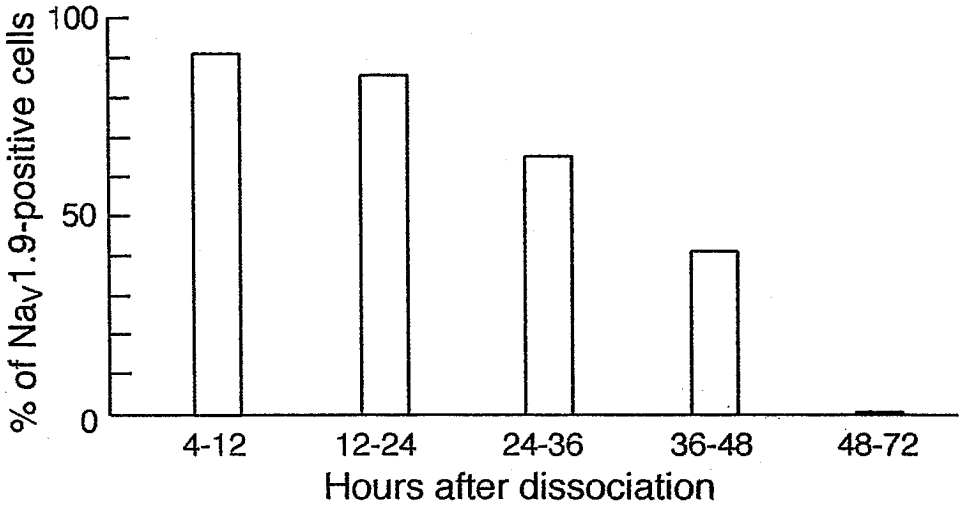
% of $Na_V1.9$-positive cells
100
50
0
4-12
12-24
24-36
36-48
48-72
Hours after dissociation

B

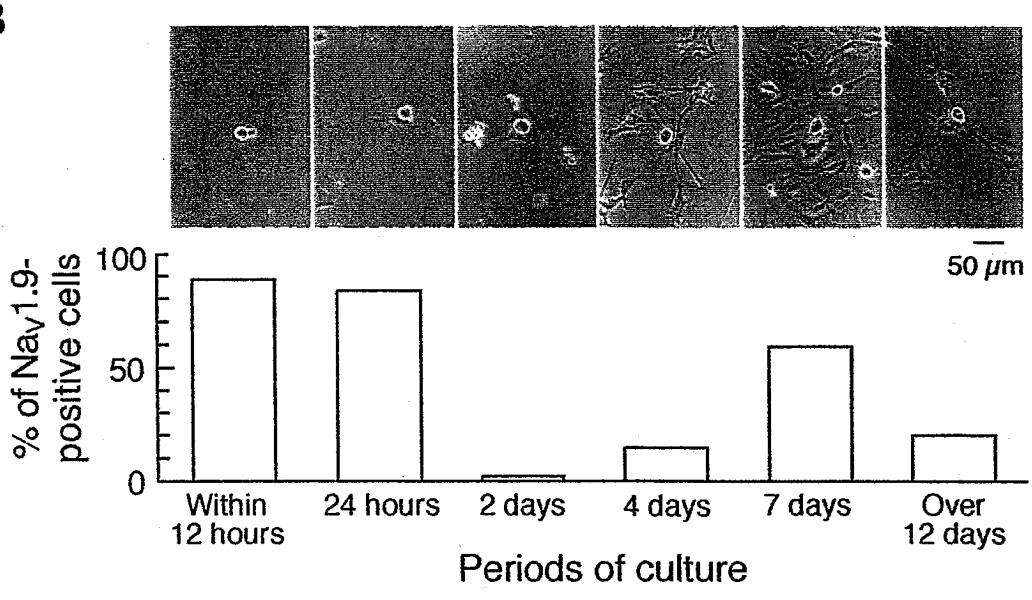
50 μm
% of $Na_V1.9$-positive cells
100
50
0
Within 12 hours
24 hours
2 days
4 days
7 days
Over 12 days
Periods of culture

Fig. 5

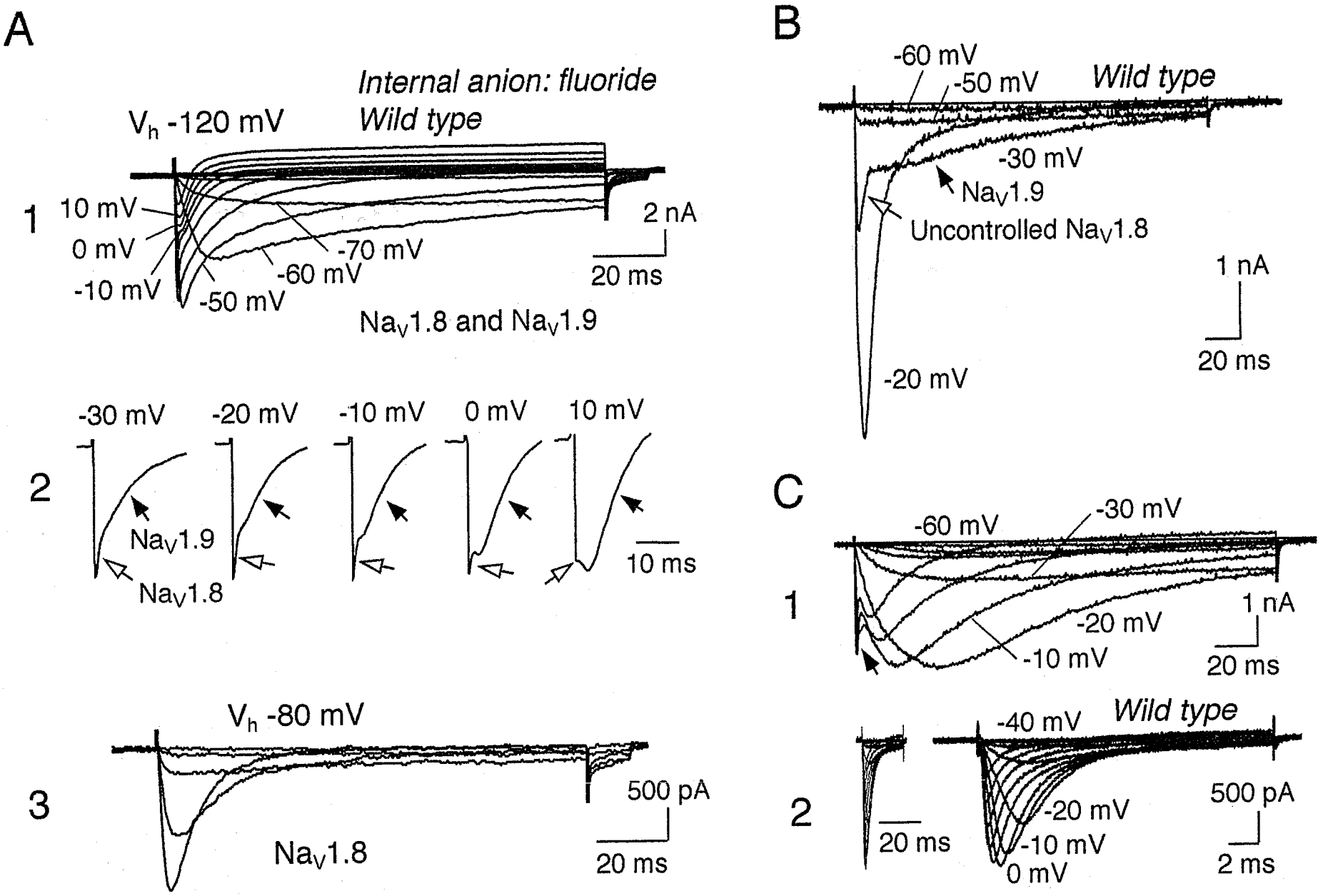
A
Internal anion: fluoride
Wild type
V_h -120 mV
1
10 mV
0 mV
-10 mV
-50 mV
-60 mV
-70 mV
2 nA
20 ms
$Na_V1.8$ and $Na_V1.9$
-30 mV
-20 mV
-10 mV
0 mV
10 mV
2
$Na_V1.9$
$Na_V1.8$
10 ms
V_h -80 mV
3
500 pA
$Na_V1.8$
20 ms
B
-60 mV
-50 mV
Wild type
-30 mV
$Na_V1.9$
Uncontrolled $Na_V1.8$
1 nA
20 ms
-20 mV
C
-60 mV
-30 mV
1
1 nA
-20 mV
-10 mV
20 ms
-40 mV
Wild type
2
20 ms
-20 mV
-10 mV
0 mV
500 pA
2 ms

Fig. 6

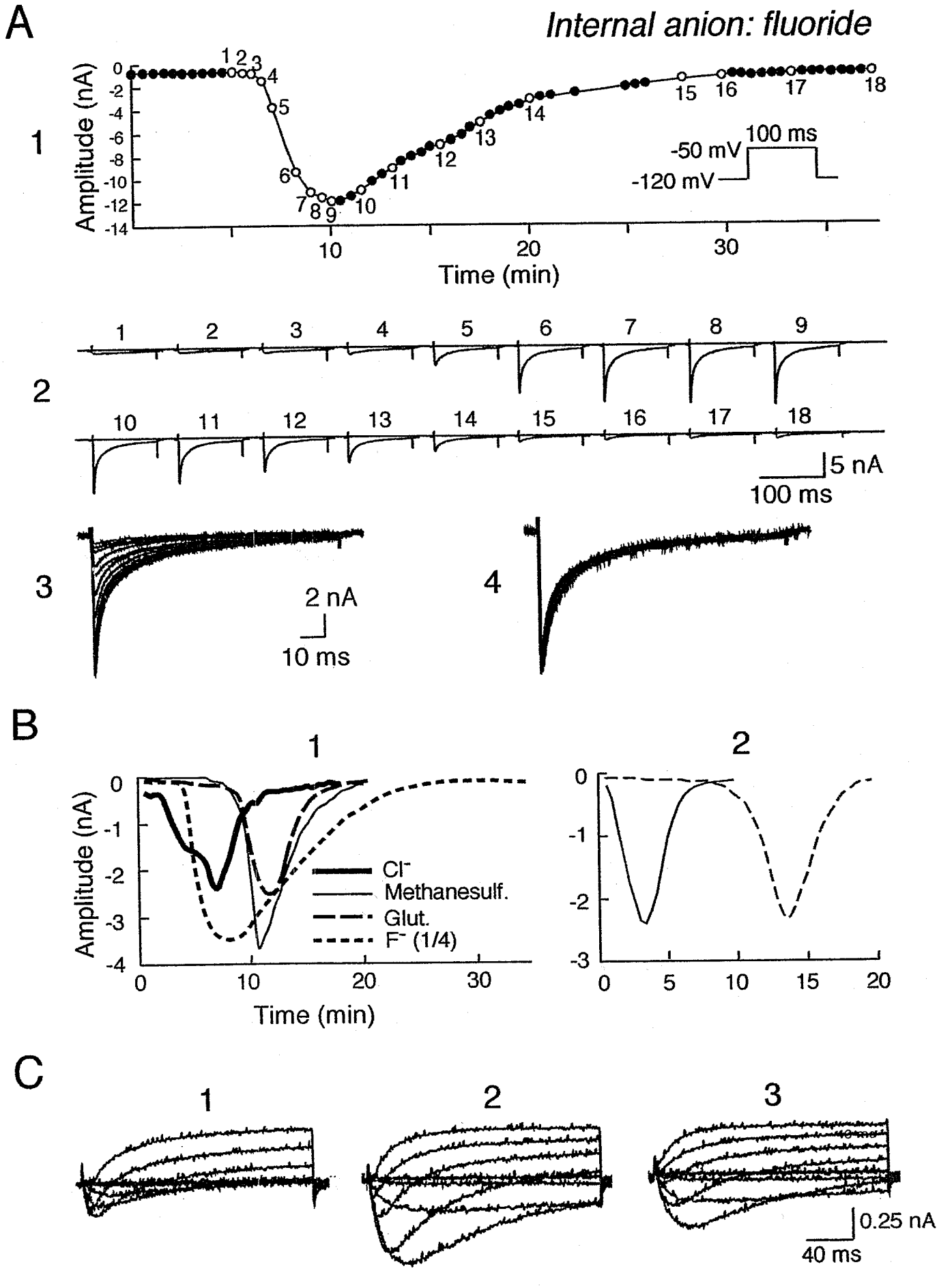
A
Internal anion: fluoride
1
Amplitude (nA)
Time (min)
-50 mV
-120 mV
100 ms
2
5 nA
100 ms
3
2 nA
10 ms
4
B
1
2
Amplitude (nA)
Time (min)
Cl⁻
Methanesulf.
Glut.
F⁻ (1/4)
C
1
2
3
0.25 nA
40 ms

Fig. 7

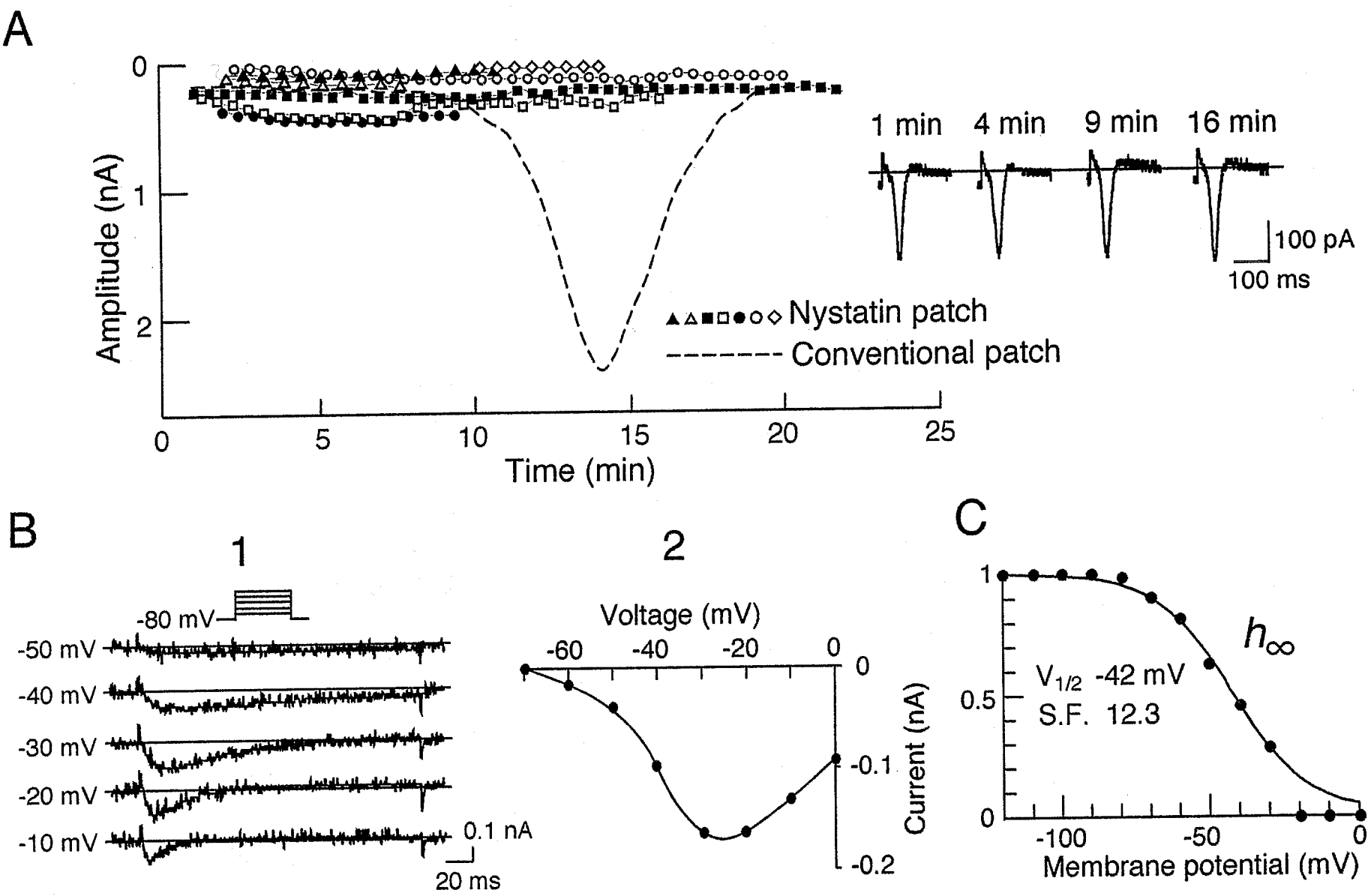
A
Amplitude (nA)
0
1
2
0
5
10
15
20
25
Time (min)
Nystatin patch
Conventional patch
1 min
4 min
9 min
16 min
100 pA
100 ms
B
1
-80 mV
-50 mV
-40 mV
-30 mV
-20 mV
-10 mV
0.1 nA
20 ms
2
Voltage (mV)
-60
-40
-20
0
0
-0.1
-0.2
Current (nA)
C
1
0.5
0
h_∞
$V_{1/2}$ -42 mV
S.F. 12.3
-100
-50
0
Membrane potential (mV)

Fig. 8

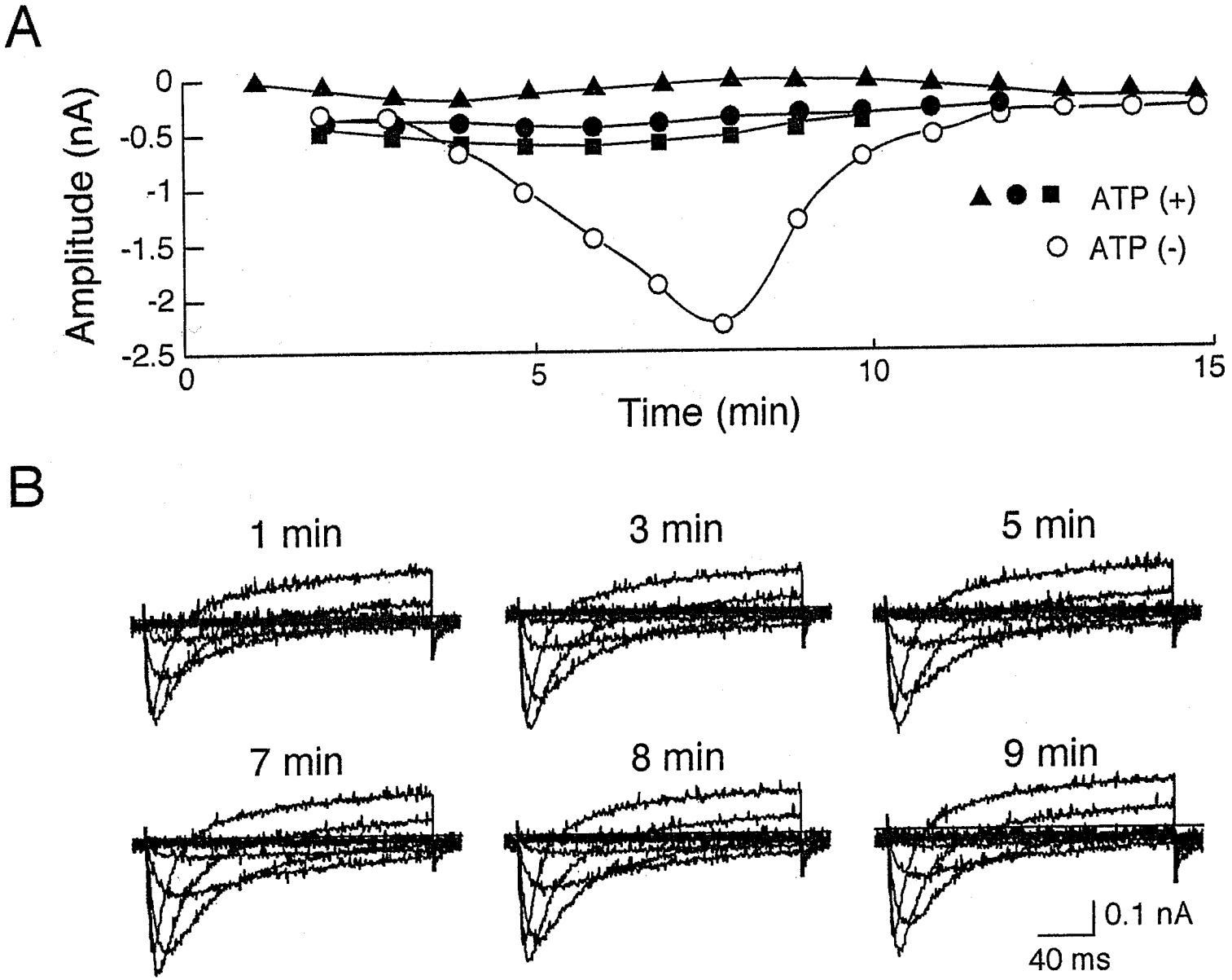
A
Amplitude (nA)
0
-0.5
-1
-1.5
-2
-2.5
0
5
10
15
Time (min)
ATP (+)
ATP (-)
B
1 min
3 min
5 min
7 min
8 min
9 min
0.1 nA
40 ms

Fig. 9